Green synthesis and characterization of silver nanoparticles using Corchorus aestuans leaf extract and their photocatalytic, antimicrobial and anti- proliferation against MCF-7 cell lines

Saravana Kumar Deivanathan
Government Arts College (Affiliated to Bharathidasan University) Tiruchirappalli
J. Thomas Joseph Prakash (armyjpr1@yahoo.co.in)
Government Arts College (Affiliated to Bharathidasan University) Tiruchirappalli

Research Article

Keywords: Corchorus aestuans, silver nanoparticles, antimicrobial properties, MB dye degradation, MCF-7 cells

Posted Date: May 23rd, 2023

DOI: https://doi.org/10.21203/rs.3.rs-2953408/v1

Abstract

The researchers are working hard to discover eco-friendly alternatives to chemically synthesized metal nanoparticles. The current study used *Corchorus aestuans* to evaluate bio-synthesis, physiochemical characterization and antimicrobial activities against human pathogenic bacteria and also the anti-cancer activity. The bio-synthesized *Corchorus aestuans* silver nanoparticles (CA-AgNPs) were characterized by UV, FT-IR, powder XRD, FE-SEM, EDAX, HR-TEM, DLS and Zeta potential. UV- Visible spectrum of the aqueous solution showed a peak at 426 nm confirming the presence of silver nanoparticles. FT-IR spectrum analysis shows the presence of functional groups. XRD spectrum shows that the bio-synthesized CA-AgNPs were crystalline in nature with a face-centered cubic structure (FCC). The TEM studies revealed that the size of the synthesized CA-AgNPs was about 13 nm. The zeta potential value of -17.9 mV exhibits those bio-synthesized nanoparticles has the excellent stability. The MTT assay also demonstrated improved cytotoxicity against bosom malignant breast cancer (MCF-7) cell lines with IC_{50} value of 56.47 µg/mL. The CA-AgNPs were also found to be anti-microbial effective against gram-positive and gram-negative bacteria and fungi. Furthermore, after 48 h of interaction, the bio-synthesized CA-AgNPs successfully degraded the Methylene blue (MB) dye nearly 91.19%.

Introduction

Nanotechnology is a rapidly expanding study field, with applications ranging from electronics to healthcare, the environment, food, textiles, and pharmaceuticals [1]. Metallic nanoparticles are a significant and vital component of nanotechnology. Metal nanoparticles are intriguing in nanotechnology due to their high surface area, low melting temperature, and optical and magnetic capabilities, to name a few. Nanotechnology combined with metal nanoparticles has been employed successfully in a variety of sectors, including biomedical sciences. Nanoparticles are used in therapy and diagnostics because of their form, size, and distinct thermal and optical properties. Metal nanoparticles' outstanding feature, which is attributable to a specific size ratio and enhanced surface area to volume, making them appropriate for various biological applications [2, 3], including theranostics [4]. As a result, nanoparticles are regarded as the foundation for the upcoming generations of photonics, semiconductors, and numerous bio- and chemical detectors [5, 6]. Whereas, both chemical chemical and physical approaches are employed to create nanoparticles, the perdurability and utilization of harmful substances is a significant problem. The use of hazardous compounds on the surface of nanoparticles in the synthesis technique restricts their usage in biotechnological and clinical applications. As a result, the development of eco-friendly, biocompatible, non-toxic and environmentally acceptable technologies for nanoparticle production is commendable [7, 8].

According to Indian Council of Medical Research (IMCR) it is estimated that approximately 162,468 new cases (87,090 deaths) of bosom malignant are diagnosed in India every year [9]. The bosom malignant development is a kind of disease that beginnings in the cells of the bosom. It can influence all kind of people, despite that the fact it is more considered normal in women. The specific reason for bosom disease is obscure, yet there are few gamble factors like age, orientation, family ancestry and openness to

estrogen [10]. Early identification and therapy are significant for the best result and choices are incorporated a medical procedure, radiation treatment, chemotherapy and chemical treatment [11, 12]. There are few issues related with the drugs in bosom malignant growth treatment. These issues contrast across individuals and between prescriptions. These types of treatment methods gives side effects in the future, so if we go for a treatment method without side effects natural medicine methods is better[13, 14].

The *Corchorus aestuans* is a shrub plant belongs to Tilliaceae family and it is grows almost near farming lands wet lands and bank of rivers. Some parts of the plants were used medicinally. It is especially used for urinary tract infections, bacterial and fungal infections.

In this research work, we successfully synthesized eco-friendly, cost effective and non-toxic AgNPs using *Corchorus aestuans* leaf extract (CALE) as a reducing agent and the products were examined by UV-visible spectra, XRD,FT-IR, HR-SEM, EDX, HR-TEM, DLS and ZETA potential. By disc diffusion method antimicrobial properties of bio-synthesized AgNPs were determined. Furthermore antioxidant, cytotoxicity and photocatalytic properties were examined.

Materials and methods

Chemicals

Silver Nitrate ($AgNO_3$) with 99.9% (Merck Life Science Pvt Ltd, Mumbai, India) purity and Methylene Blue (MB) were purchased from Merck specialties Pvt Ltd, Mumbai, India and the purchased chemicals are used without any purification. All the experiment was carried out through ultrapure de-ionized water.

Preparation of CALE

The *Corchorus aestuans* (CA) leaf were collected from Puliyancholai, Tiruchirappalli, Tamil Nadu, washed thoroughly with fresh water to remove unwanted dirt and finally rinsed with ultrapure de-ionized water for many times; further, the washed *C.aestuans* leaves are dried in shadow and finally grinded into powdered form. A 2 g of *C.aestuans* leaves powder was taken into 200 mL beaker with 100 mL ultrapure de-ionized water. The CA leaves allowed to soaking for 20 min. Then the solution was kept in a heating mantle at 60°C until get the pungent smell. The boiled solution of *Corchorus aestuans* leaf extract (CALE) was allowed to cool and filtered with whatman No.1 filter paper, refrigerated at 4°C for future use.

Synthesis of AgNPs by CALE

In a 200 mL of beaker, 90 mL of $AgNO_3$ solution (1 mM) and the CALE solution of 10 mL are added together and the mixture was stirred for an hour. The bio-synthesized AgNPs were centrifuged at 10,000 rpm for 20 minutes for using Remi 12 C machine. Finally the reduced the AgNPs solution was dried and powdered to further characterizations studies.

Characterization studies of biosynthesized AgNPs

After the synthesis process take place, the AgNPs were undergone to various physiochemical characterization studies. The spectral analysis of the bio-synthesized AgNPs is studied with UV-visible spectrometer (model: Perkin Elmer lambda 35). The functional group present in the synthesized AgNPs was carried out by FT-IR Spectrometer with range 4000 – 400 cm^{-1}. The synthesized AgNPs size was assessed by using HR-TEM (JEOL-2100 model) with resolution 0.194 nm. The surface morphological studies and EDAX were found out by utilizing HR-SEM (Quanta FEG 250). The hydrodynamic size and the stability of the synthesized AgNPs solution are investigated by DLS-Zeta potential (ZS-90, Malvern UK 2012 model). The crystallite size of the AgNPs was examined by Powder X-Ray Crystallography (Bruker Model).

Photocatalytic activities- MB dye degradation

To make a stock solution, dissolve 5 mg of MB (Methylene Blue) in 500 ml of de-ionized water. That MB stock solution contains about 5 mg of biosynthesized AgNPs. A few milliliters of control solution are preserved without the addition of MB. The solution was mixed for an hour using Remi 2MLH magnetic stirrer to ensure that the working solution was clearly balanced. Furthermore, the produced solution was exposed to sunlight and the changes were observed from sunrise to sunset. A 3 ml sample of the mixture was obtained and centrifuged at regular intervals to analyze the photocatalytic dye degradation. The residual absorption spectra were then analyzed using UV-vis spectroscopy at various wavelengths. The absorbance value at 660 nm was used to estimate dye concentration throughout disintegration.

The percentage of dye degradation is calculated by using the formula:

$$\text{Dye degradation \%} = \frac{C0-C}{C0} \times 100$$

Here, C_0 is the initial concentration of the dye solution and C is the concentration the dye solution after photocatalytic degradation.

Anti-microbial activities

The objective of this research has been to look at the anti-bacterial and anti-fungal activities of biosynthesized CA-AgNPs against various pathogens utilizing the disc diffusion methods. The anti-bacterial activities anti-fungal activities of CA-AgNPs sample were exposed to two gram positive bacterial strains, *Staphylococcus aureus* (MTCC 25923) and *Bacilius subtilis* (MTCC 2451) and two gram negative bacterial strains, *Escherichia coli* (MTCC 25922) and *Streptococcus aureus* (MTCC 2451). The Microbial Type Culture and Collection (MTCC) in chandigarh, India, provided all of the bacterial strains. The Kirby-bauer disc diffusion technique was used to assess the antimicrobial effects of CA-AgNPs. Mueller-Hinton agar was used to produce the petri dishes diameter about 60 mm which were then injected with tested microorganisms. Sterile discs of six mm width were treated with 10 µL of each sample. The prepared discs were put on the outermost surface of the agar plates and kept at ambient temperature for half an hour to permit compound diffusion. The positive control was made using 10 µL of amoxicillin as the typical antibiotic disc. The plates are incubated at 37°C for 24 h and the zone of inhibition was measured in mm. The experiment was done twice.

Anti-oxidant activities

The stable DPPH (2,2-diphenyl-1-picrylhydrazyl) free radical activity was used to assess the antioxidant activity of the bio-synthesized CA-AgNPs sample. A 300 µL ethanolic solution of DPPH (0.05 mM) was introduced to 1000 µL of bio-synthesized AgNPs at various quantities (100–500 µL). The newly prepared DPPH solution was stored at 4°C in the dark. The mixture was then shaken with 96% (2.7 mL) of ethanol. After 5 minutes of standing at 540 nm, the absorption was determined spectrophotometrically. Using ethanol, absorbance was set to zero. A blank sample contains the same amount of ethanol and DPPH was prepared. All these were performed in triplicate. The free radical activity of the tested samples expressed as a percentage of inhibition was calculated.

DPPH activity inhibition % = $\frac{A-B}{A} \times 100$.

Where, A and B represent the absorbance readings of the baseline and sample correspondingly.

Cytotoxicity analysis

Using MCF- cells, the CA-AgNPs sample was evaluated fro in-vitro cytotoxicity using the 3-(4,5-dimethylthiazol-2-yl)-2,5-diphenyltetrazolium bromide(MTT) assay. In brief, trypsinization was used to extract MCF- cells, which were then combined in a 15 mL container. The cells were then plated into 96-well tissue culture plates at a density 1×10^5 cells/mL cells/well (200 µL) into 96-well tissue culture plate in DMEM medium containing 10% FBS and 1% antibiotic solution for 24–48 h at 37°C. The wells were washed with sterile PBS before being treated in a serum-free DMEM medium with various concentration of the CA-AgNPs sample.

Statistical analysis

All results were provided as mean standard deviations, with significance set at $P \leq 0.05$ for statistical analysis of variance (ANOVA). SPSS 20.0 was employed and followed by turkey's range test.

Result and discussions

UV-Vis spectra analysis of bio-synthesized CA-AgNPs

After thorough mixing in the precursor solution, a significant visual shift of colour from light brown to dark brown was seen, confirming the existence of AgNPs. The UV- visible absorption spectrum shows the absorption peak at 440 nm (Fig. 1) confirms the silver in the nanoscale range and the surface plasmon resonance (SPR) band corresponds to spherical in nature [15]. The reduction of Ag^+ ions into Ag^0 metal by the bio-products present in the leaf extract. [16, 17].

FT-IR analysis of bio-synthesized CA-AgNPs

The Fig. 2 depicts the FT-IR profile of the bio-synthesized CA-AgNPs. The FTIR spectra revealed notable peak at 3444 cm^{-1} corresponds to OH - stretching due to alcoholic group [18]. The peak at 2992 cm^{-1} corresponds to H-C-H of amines and the peak at 2884 cm^{-1} is corresponds to C-H stretch of alkanes [19]. The peak at 2082 cm^{-1} is corresponds to alkyne group present in the bio-products of plant leaves [20] and the peak at 462 cm^{-1} is corresponds to C-O stretching of acetyl groups and belongs to amides [21]. The peaks at 1264 cm^{-1} is corresponds to C-N stretching and it belongs to aliphatic amines [22]. The peak at 1040 cm^{-1} is corresponds to S = O stretching, sulfoxide characteristics [23], and the peak at 882 $cm^{-1}$and 692 cm^{-1} is = C-H bending of Alkenes [24].

Powder XRD- analysis of bio-synthesized CA-AgNPs

The Powder XRD technique was used to analyze the crystalline structure of the synthesized AgNPs. The Fig. 3 shows the Powder XRD plot of the bio-synthesized AgNPs by *C.aestuans* leaf crude extract. From the plot, it shows the four strong peaks at different angles as 38.24°, 44.36°, 64.53°,77.48° which are corresponds to (111), (200), (220) and (311) planes respectively and it indicates the face centered cubic (FCC) nature of the crystal. Using scherrer's equation $D = k\lambda/\beta\cos\theta$, where θ is the diffraction angle of the peak, β is the FWHM value, λ is the wavelength of the incident X-rays, from these values, average size of the crystallite was determined as 20.64 nm, which has the good agreement with TEM histogram result [25–28]. Some of the undesirable peaks indicates the presence biomolecule compounds of *C.aestuans* plant leaves [29, 30]. The crystallographic plot was drawn with origin 2018 software and Xpert High Score Plus.

HR-SEM and TEM and EDAX analysis bio-synthesized CA-AgNPs

The Fig. 4 shows, HR-SEM images of the bio-synthesized CA-AgNPs at various magnifications with EDAX analysis. The EDAX spectrum shows an Ag signal at 3.0 KeV [31] with of 70.3% of Ag. Furthermore, Oxygen, Silicon and Chlorine were at 21.3%, 1.8% and 2.7% respectively.

The surface morphologies of bio-synthesized CA-AgNPs were characterised by HR-TEM. From the image (Fig. 5), these bio-synthesized CA-AgNPs were predominantly spherical in form; the SAED pattern of the bio-synthesized CA-AgNPs confirmed the crystallinity nature of nanoparticles [32]. The particles histogram revealed an average diameter of about 12.5 nm which has close to crystallite size by Scherer's equation.

DLS and ZETA potential analysis

Dynamic Light Scattering is a non-invasive technique that can be used to measure particles in a wide range of samples types, including polymers, proteins, liposomes and nanoparticles. DLS is particularly useful for measuring particles in the nanometre range, wherever other techniques such as microscopy may not be suitable [21, 33]. DLS can identify the size distribution of the particles in suspension using autocorrelation methods. The size distribution is typically presented as a single value such as the polydispersity index's mean size (PDI). For this bio-synthesized solution, the PDI value is 0.261 that they

are monodispersed with particle size ranges from 6.8 nm to 116.3 nm (Fig. 6-a) and the average size of the particles is 105.5 nm. The magnitude and sign of the zeta potential are affected by particle and fluid characteristics such as pH, ionic strength, composition and temperature. The ZETA potential (electro kinetic potential) value of the bio-synthesized CA-AgNPs is -14.1 mV (Fig. 6-b) which indicates that the bio-synthesized CA-AgNPs has the strong stability [34].

MB dye degradation of bio-synthesized CA-AgNPs

The dye MB was used to illustrate the photocatalytic activity of AgNPs on dye degradation. MB was degraded in the presence of AgNPs at a different time in the visible sunlight. At various time intervals, the absorption spectra revealed decreasing peaks for MB. Initially, the absorption peak at 660 nm for MB dye steadily diminished with increasing exposure duration, indicating MB photocatalytic degradation [35, 36]. Following that, the blue colour was turned into light bluish green (Fig. 7 inside picture). Finally, the degradation process was finished at 72 h, as indicated by a shift in the coloring of the dye solution to colourless. The adsorption of AgNPs in MB solution began slowly and gradually increased with increasing time and dye degradation percentage [37, 38].

The degradation efficiency was assessed using the $-\ln(C_0/C)$ curve which is depicted in Fig. 7. The Co and C represent the dye concentration at time t = 0 and t respectively. The dye concentration with in the solution at any given moment may be calculated using this graph. The sample had the maximum degradation efficiency with approximately 9% of dye remaining in the solution at the end of the photocatalytic process (Fig. 8 inside pic). This research demonstrates that CA-AgNPs have the capability to play a role in the environmental treatment for the creation of nanocatalysts.

Antimicrobial assay

In this present research work the antibacterial effects of bio-synthesized CA-AgNPs on two gram positive bacterial strains *Staphylococcus aureus* (MTCC 25923), Bacillus subtilis (MTCC 2451) and two gram negative bacterial strains *Escherichia coli* (MTCC 25922), *Streptococcus aureus* (MTCC 2451) were investigated. The Fig. 9 depicts the inhibition zone surrounding each well. The exact value of the created zone, as well as antibiotic control Amoxicillin is provided. From the obtained values, Bacillus subtilis (MTCC 2451), *Escherichia coli* (MTCC 25922) and *Streptococcus aureus* (MTCC 2451) were determined to be 6 ± 0.8165 mm, 7 ± 1.8257 mm and 5 ± 0.8165 mm of inhibition zone respectively (Table No.1). Comparing with other bacteria, the *Staphylococcus aureus* (MTCC 25923) did not reacted well.

Table.1 Antibacterial activities of bio-synthesized CA-AgNPs with their inhibition zone values.

amples	Concentrations (µL/mL)	Organisms/Zone of inhibition (mm)			
		Staphylococcus aureus	*Bacillus subtilis*	*Escherichia coli*	*Streptococcus aureus*
(Amoxicillin)	10	6±0.8165	8±0.8165	8±1.8251	7±0.8165
(silver)	10	0±0.0000	0±0.0000	0±0.0000	0±0.0000
(Plant xtract)	10	0±0.0000	2±1.6329	3±1.8257	2±0.8165
	10	0±0.0000	6±0.8165	7±1.8257	5±0.8165
Nanoparticles)					

Anti-fungal assay.

The Fig. 10 depicts antifungal test finding for biosynthesized CA-AgNPs. It is seen that the bio-synthesized CA-AgNPs are more effectively responded with *Aspergillus flavus* (4 ± 0.8165 mm) than *Aspergillus niger* (1 ± 0.8165 mm). Besides that, the pure leaves extract of C.aestuans alone was efficacious against *Aspergillus flavus* (2 ± 0.8165 mm) whereas, it was ineffective against *Aspergillus niger*. According to the earlier studies the existence of bio-products in C.aestuans was mainly accountable for the antifungal activity. In this research work C.aestuans leaves extract with silver nitrate showed excellent antifungal potential [39, 40]. Here, fluconazole has taken as control and Table.2 shows the zone if inhibition in mm.

Table.2 Anti-fungal activities of CA-AgNPs with their inhibition zone.

Samples	Concentrations (µl/ml)	Organisms/Zone of inhibition (mm)	
		Aspergillus flavus	*Aspergillus niger*
A (Fluconazole)	10 µl	8±1.8257	7±1.8257
B (Silver)	10 µl	0±0.0000	0±0.0000
C (Plant extract)	10 µl	2±0.8165	0±0.0000
D (Nanoparticles)	10 µl	4±0.8165	1±0.8165

Anti-oxidant

The DPPH (2,2-diphenyl-1-picrylhydrazyl) assay was used to determine the anti-oxidant activity of the bio-synthesized CA-AgNPs. Many studies have been conducted to explore antioxidant activities of silver nanoparticles and it has been discovered that they have amazing antioxidant properties and the bio

products like phenolic were present in the leaf extract were responsible for the antioxidant behaviour [41–43]. The antioxidant test findings for CA-AgNPs at 100, 200, 300, 400 and 500 µg/mL were 63.24 ± 0.83283, 67.23 ± 1.84409, 70.76 ± 1.64932, 74.58 ± 1.844 and 77.64 ± 0.82466% respectively (Table.3). From these analyses when the concentration of CA-AgNPs increased, it also increases the antioxidant values (Fig. 11) [44].

Table.3 Compression of CA-AgNPs with Ascorbic acid and their Inhibition zone

S.NO	CONCENTRATION (µg/mL)	DPPH activity inhibition %	
		CA-AgNPs	Ascorbic Acid
1.	100	63.24 ± 0.83283	71.73 ± 1.84409
2.	200	67.23 ± 1.84409	75.45 ± 2.59493
3.	300	70.76 ± 1.64932	79.84 ± 1.84400
4.	400	74.58 ± 1.84400	83.46 ± 0.83283
5.	500	77.64 ± 0.82466	89.63 ± 1.81485

Cytotoxicity analysis of bio-synthesized CA-AgNPs.

The AgNPs have been widely used in medicine, because of their great anti-cancer potential. AgNPs produced by bio-synthesis has the ability to inhibit cell growth and induce cell death [45]. This study looks at the anticancer effects on CA-AgNPs of human breast cancer cells. The bio-synthesized CA-AgNPs degrade the DNA and cause cell death. In this current work, the cytotoxicity impact of CA-AgNPs was investigated against human breast carcinomas cells (MCF-7) using MTT assay. On the observation of 24 h, the survivability of cancer cells diminished as the quantity of CA-AgNPs increased (Fig. 13). Furthermore, a considerable change in the structure, such as degradation of membrane fluidity, reduced cell size, and shrinkage in cell structure (Fig. 12) showed that the bio-synthesized CA-AgNPs may have anticancer properties [46–49].

Conclusion

This profitable and eco-friendly approach might possibly be used for large-scale synthesis of AgNPs. FT-IR spectroscopic study of the leaf extract found the bio-products were responsible for reduction and stabilizing of AgNPs. UV-vis, Powder XRD, HR-TEM, DLS and ZETA potential were used to describe the metal nanoparticles. Thus, the result shows that bio-synthesized AgNPs from *Corchorus aestuans* leaf extract have a significant anticancer activity with apoptotic features and the current findings suggest that CA-AgNPs could contribute to the advancement of a specific anti-cancer drug, paving the way for the development of novel nano-medicines for the treatment of cancer and microbial contagious disease. The primary absorption peak at 660 nm steadily diminished with increasing exposure duration, suggesting dye degradation of methylene blue. The use of natural and eco-friendly reducing for the synthesis of

silver nanoparticles shows outstanding degradation activity against dye content and may be employed in purifying water systems and dye effluent remediation, according to the findings of this research.

Declarations

Ethical Approval

We also declare that the study was performed according to the international, national and intuitional rules considering animal experiments, clinical studies and biodiversity rights. And also no animals / humans were harmed in this research work.

Competing interests

The authors declare that they have no competing interest.

Author's contributions

Authors

We confirm that the manuscript has been read and approved by all named authors and that there are no other persons who satisfied the criteria for authorship but are not listed. We further confirm that the order of authors listed in the manuscript has been approved by all of us.

Funding

This research did not receive any specific grant from funding agencies in the public, commercial, or not-for-profit sectors.

Availability of Data and Materials

The data that support the findings of this study are available from the corresponding author [J TJ Prakash] upon reasonable request.

Corresponding Author

We understand that the Corresponding Author is the sole contact for the Editorial process. He is responsible for communicating with the other authors about progress, submissions of revisions and final approval of proofs

Copyright and Plagiarism

We declare that this manuscript is original, has not been published before and is not currently being considered for publication elsewhere.

Acknowledgment

The authors express his gratitude to Mr. Nirmal Kumar .R and Ms. Megaraj Begam, Research Scholar, NIT, Tiruchirappalli and Dr. A. Kalpana., Asst Prof. of Chemistry, Government Arts College, Tiruchirappalli-22.

References

1. Bedlovicova Z, Strapac I, Balaz M, Salayova A. Molecules **25** (2020).
2. Suresh Babu Naidu K, Murugan N, Adam J K, Sershen BioNanoscience **9** (2019)266 273.
3. Annavaram V, Posa V R, Uppara V G, Jorepalli S, Somala A R BioNanoscience **5** (2015) 97-103.
4. Chen F, Ehlerding E B, Cai W. J Nucl Med **55** (2014) 1919 1922.
5. Lee S H, Jun B- H Int J Mol Sci **20** (2019).
6. Shiju E, Sharafudeen K, Remya T M, Siji Narendran N K, Sudheesh P, Sadasivan Nair V *Photonics* **8** (2021).
7. Huang L, Sun Y, Mahmud S, Liu H. J Inorg Organomet Polym Mater **30** (2020).
8. Bhardwaj B, Singh P, Kumar A, Kumar S, Budhwar V Adv Pharm Bull **10** (2020).
9. Viral P, Pavithran K, Beena K, Shaji A, Vijayakumar D K J Carcinog **20** (2021).
10. Mathur P, Sathishkumar K, Chaturvedi M, Das P, Sudarshan K L, Santhappan S, Nallasamy V, John A, Narasimhan S, Roselind F S. JCO Glob Oncol **6** (2020) 1063-1075.
11. Sathiskumar K, Chaturvedi M, Priyanka Das, Stephen S, Mathur P Indian J Med Res **156** (2022) 598-607.
12. Nguyen N T T, Nguyen L M, Nguyen T T T, Nguyen T T, Nguyen D T C, Tran T V Environ Chem Lett **20** (2022) 253-2571.
13. Azim H A, de Azambuja E, Colozza M, Bines J, Piccart M J. Ann Oncol **22** (2011) 1939-1947.
14. Kim J W, Lim A, Lee J Y, Choi Y J, Kim Y H, Park K H. Ann Oncol **33** (2022).
15. Sreekanth T V M, Pandurangan M, Kim D H, Lee Y R J Cust Sci 27 (2016) 671–681.
16. Anand K, Kaviyarsasu K, Muniyasamy S, Roopan S M, Gengan R M, Chuturgoon A A J Clust Sci **28** (2017) 2279–2291.
17. Panda M K, Dhal N K, Kumar M, Mishra P M, Behera R K Mater Today: Proc **35** (2021).
18. Patil M P, Rokade A A, Ngabire D, Kim G -D. J Clust Sci **27** (2016).
19. Karthik L, Gaurav Kumar, Vishnu Kirthi A, Rahuman A A, Bhaskara Rao K V. Bioprocess Biosyst Eng **37** (2014).
20. Rani R, Sharma D, Chaturvedi M, Yadav J P Chem Pap **74** (2020)1817-1830.
21. Mohammadalineejhad S, Almasi H, Esmaiili M Mater Sci Eng C **105** (2019).
22. Ahamed S, Saifullah, Ahamed M, Swami B L, Ikram S. J Radiat Res Appl Sci 9 (2016).
23. Benakashani F, Allafchian A R, Jalali S A H. Karbala Int J Mod Sci **2** (2016).
24. Moteriya P, Padalia H, Chanda S. J Genet Eng Biotechnol **15** (2017) 505-513.

25. Shameli K, Ahmad M B, Zamanian A, Sangpour P, Shabanzadeh P, Abdollahi Y, Zargar M. Int J Nanomedicine **7** (2012) 5603-5610.
26. Panja S, Chaudhuri I, Khanra K, Battacharyya N. Asian Pac J Trop Dis **6** (2016) 549-556.
27. Al-Ansari M M, Dhasarathan P, Ranjitsingh A J A, Al-Humaid L A. Saudi J Biol Sci **27** (2020) 2993 3002.
28. Elumalai D, Hemavathi M, Vijayalakshmi Deepaa C, Kaleena P K. Parasite Epidemiol Control **2** (2017) 15 26.
29. Ajitha B, Ashok Kumar Reddy Y, Rajesh K M, Sreedhara Reddy P. Mater Today Proc **3** (2016) 1977 1984.
30. A Dashora, K Rathore, S Raj, Kanika Biochem. Biophys Rep **31** (2022) 101320.
31. Patil M P, Rokade A A, Ngabire D, Kim G –D. J Clust Sci **27** (2016) 1737 1750.
32. Tripathy D, Modi A, Narayan G, Rai S P. Mater Sci Eng C **100** (2019).
33. Stetefeld J, McKenna S A, Patel T R. Biophys Rev **8** (2016).
34. Jemilugba O T, Mamour Sakho E H, Parani S, Mavumengwana V, Oluwafemi O S. Colloid Interface Sci Commun **31** (2019)100191.
35. Safa M M, Merouane F, Messaad C E H, Golzadeh N, Vasseghian Y, Berkani M. Environ Res **204** (2022) 112360.
36. Al-Zaban M I, Mahmoud M A, AlHarbi M A. Saudi J Biol Sci. **20** (2021).
37. Kadam J, Dhawal P, Barve S, Kakodar S (2020). SN Appl Sci 2.
38. Vidhu V K, Philip D Micron **56** (2014).
39. Biswas C, Dey P, Satpathy S, Satya P. BioControl **57** (2012) 565-571.
40. Ahmed F. Pharmacogn Res **13** (2021)
41. Acharya K, Samui K, Rai M Ind Jr Exp Biol **42** (2004).
42. Eva Stefanovits-Banyai, Maria H. Tulok, Attila Hegedus, Csilla Renner, Ilona Szollosi Varga. Acta Biologica Szegediensis **47** (2003).
43. Lateef A, Oladejo S M, Akinola P O, Anina D A, Beukes L S, Folarin B I, Gueguim-Kana E B *Mater Sci Eng* **805** (2020) 012042.
44. Maheshwaran G, Nivedhitha Bharathi A, Malai Selvi M, Krishna Kumar M, Mohan Kumar R, Sudhahar S Green. J Environ Chem Eng **8** (2020)104137.
45. Jannathul Firdhouse M, Lalitha P. Prog Biomater **4** (2015) 113-121.
46. Gomathi A C, Xavier Rajarathinam S R, Mohammed sadiq A, Rajeshkumar S. J Drug Deliv Sci Technol **55** (2020).
47. Sahin B, Demir E, Aygun A, Gunduz H, Sen F. J Biotechnol **260** (2017).
48. Almalki M A, Khalifa A Y Z J Photochem Photobiol B: Biol **204** (2020) 111786.
49. Sadat Shandiz S A, Shafiee Ardestani M, Shahbazzadeh D, Assadi A, Ahangari Cohan R, Asgary V, Salehi S. Artif Cells Nanomed Biotechnol **45** (2017).

Figures

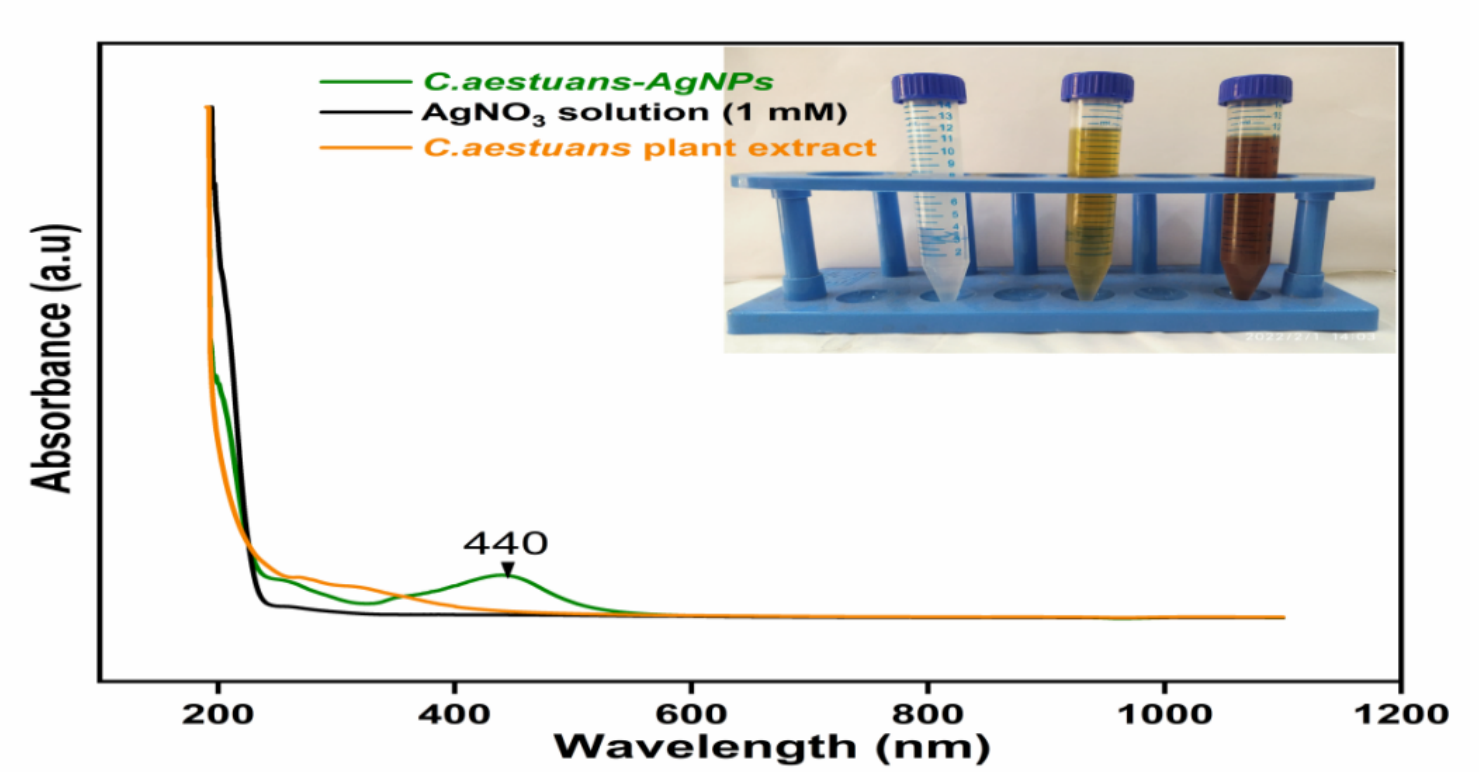

Figure 1

UV- vis profile of bio-synthesized CA-AgNPs, $AgNO_3$ solution and *C.aestuans* leaf extract.

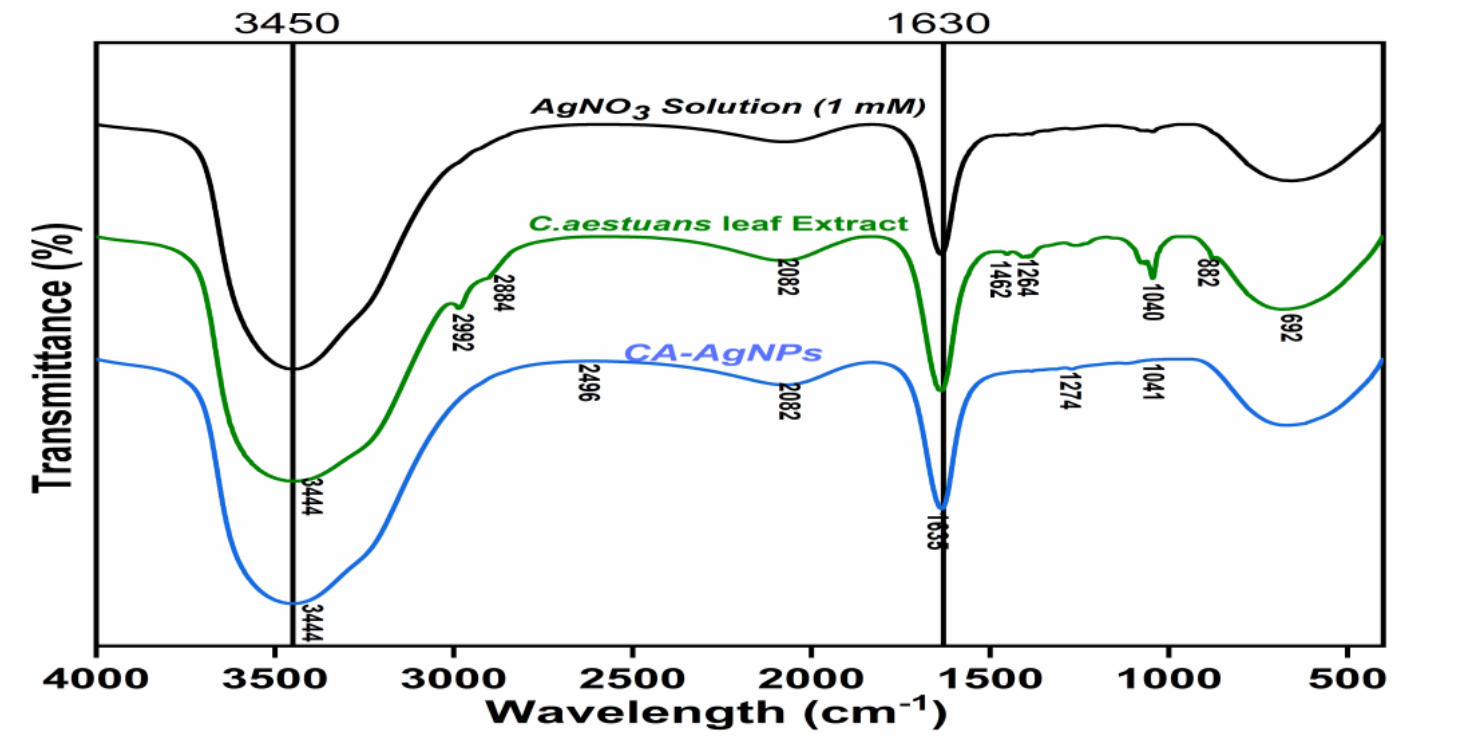

Figure 2

FT-IR profile of $AgNO_3$ Solution, *C.aestuans* leaf extract and bio-synthesized CA-AgNPs

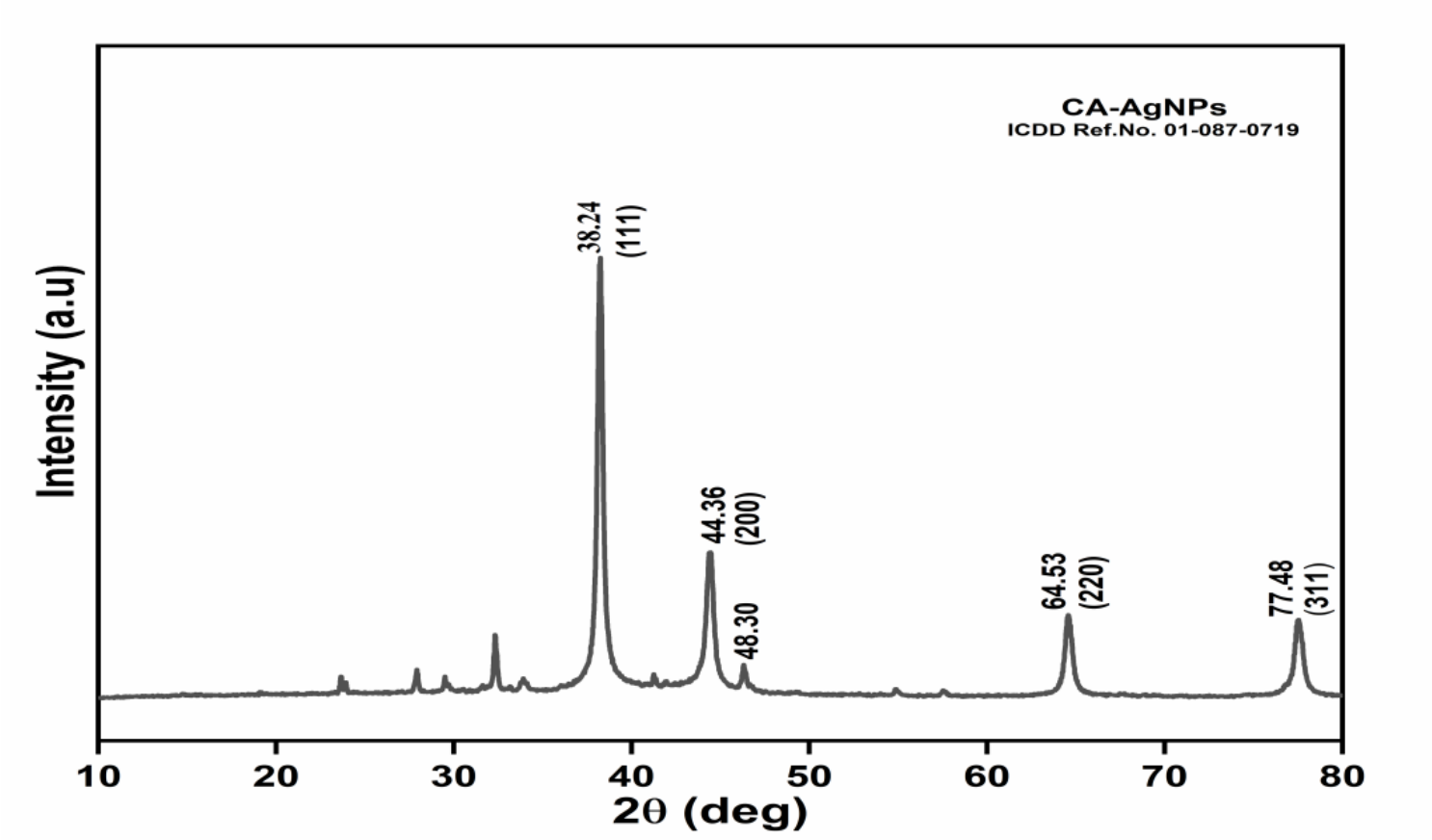

Figure 3

Powder XRD-profile of bio-synthesized CA-AgNPs.

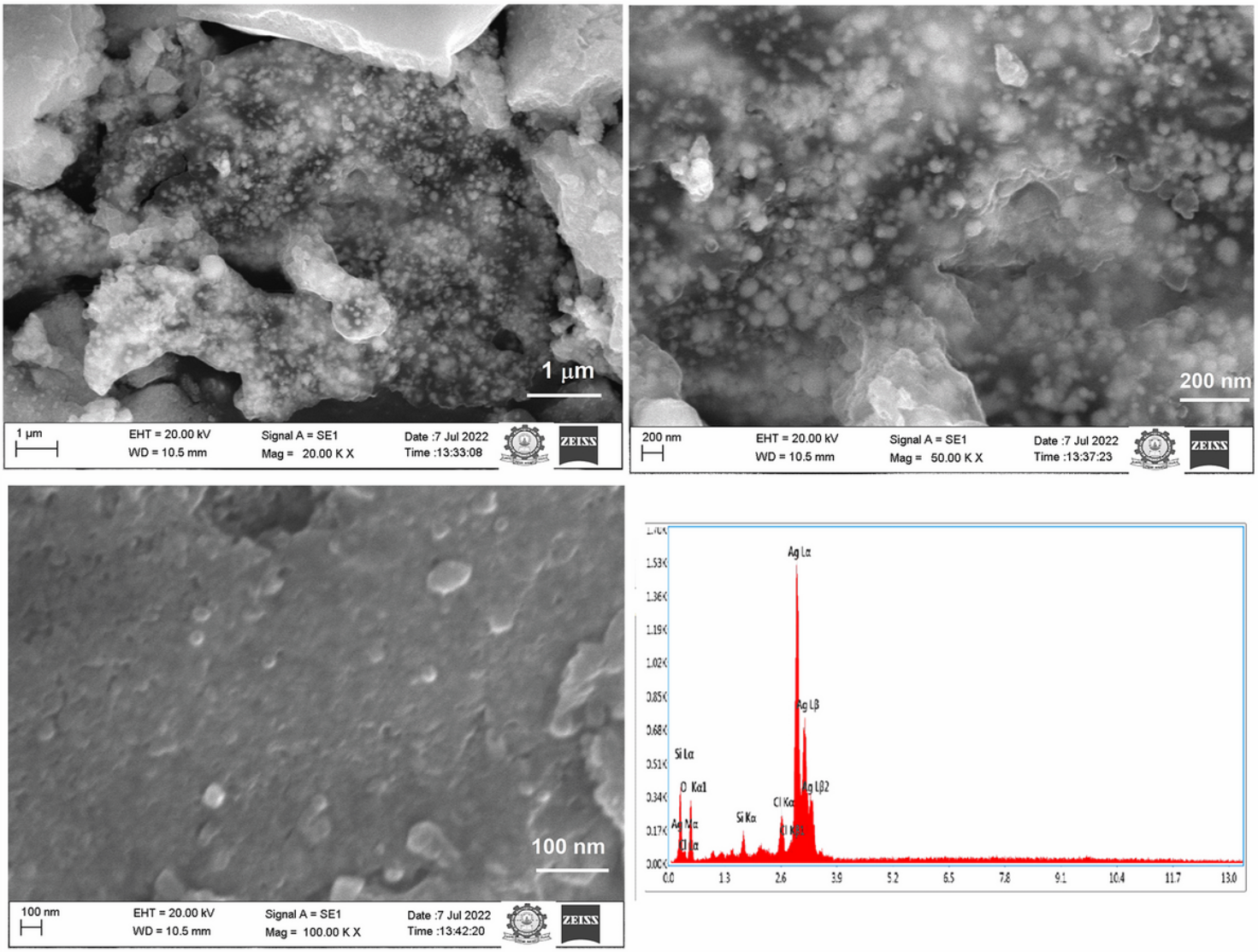

Figure 4

HR-SEM images of CA-AgNPs at various magnifications.

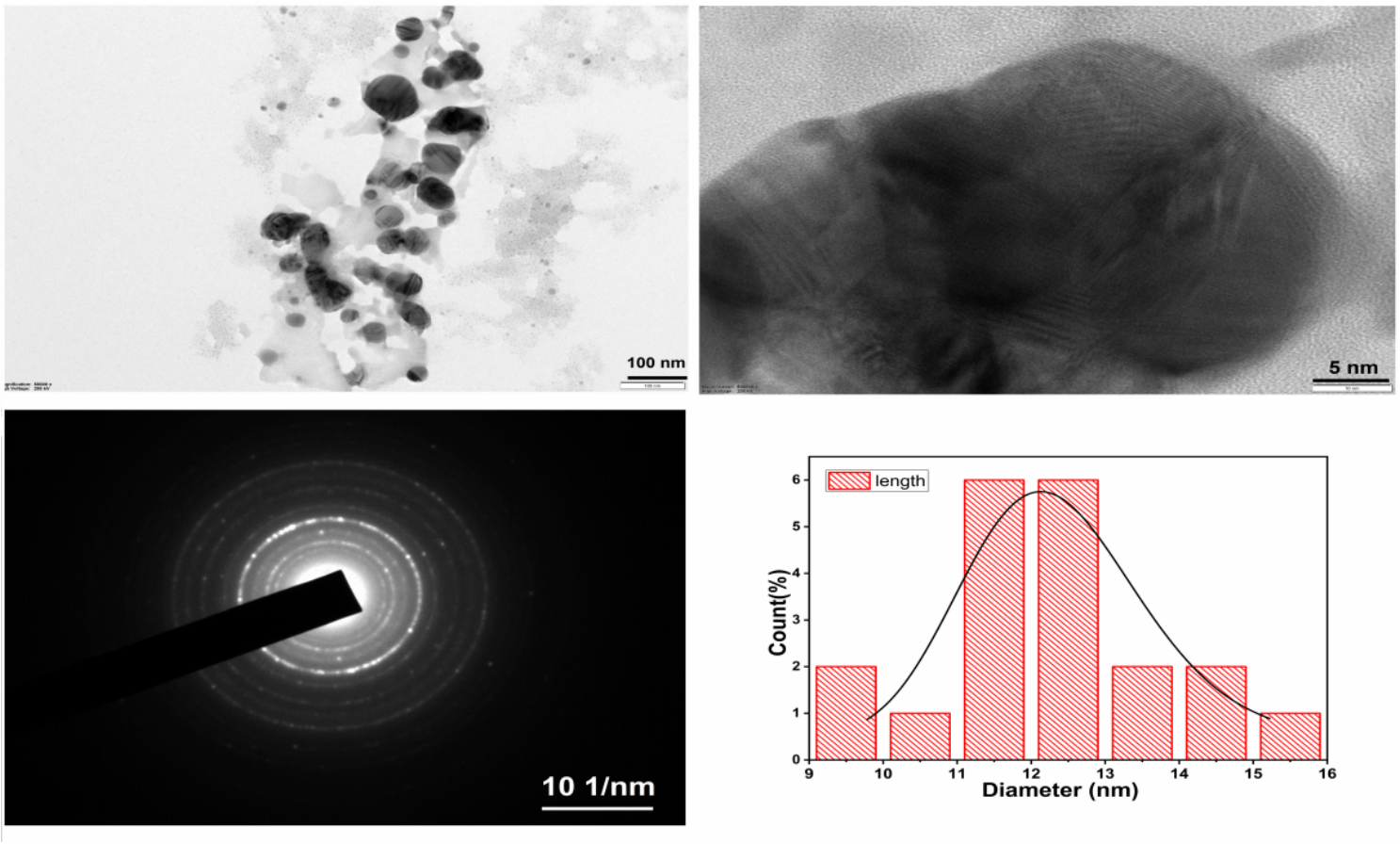

Figure 5

HR-TEM images of CA-AgNPs at various magnification and histogram graph.

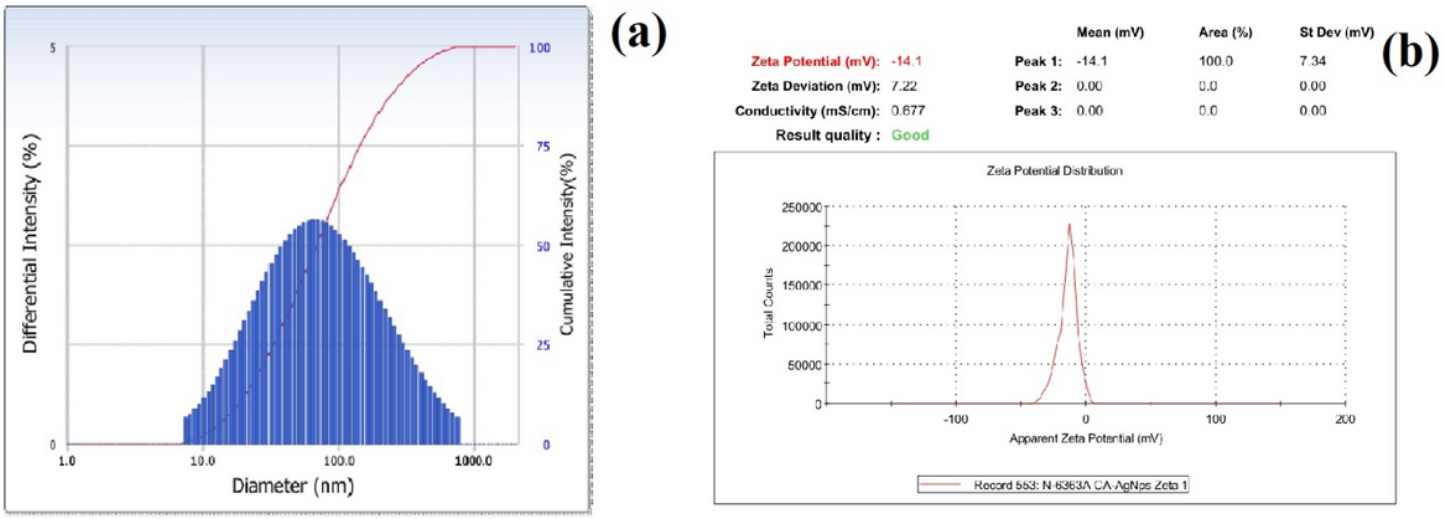

Figure 6

(a) DLS profile of CA-AgNPs and (b) Zeta Potentials analysis of CA-AgNPs

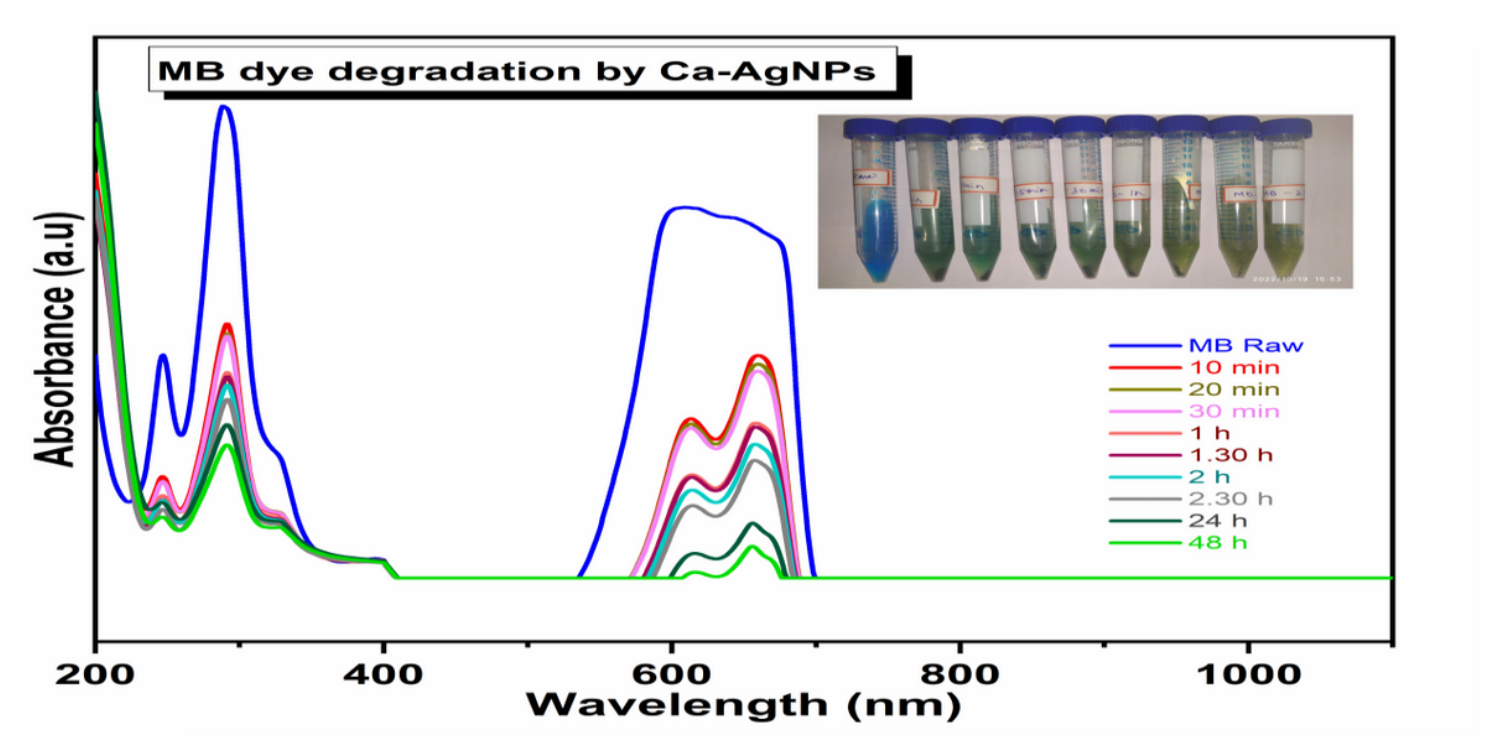

Figure 7

UV- Vis spectra of MB dye vs bio-synthesized CA-AgNPs at different time.

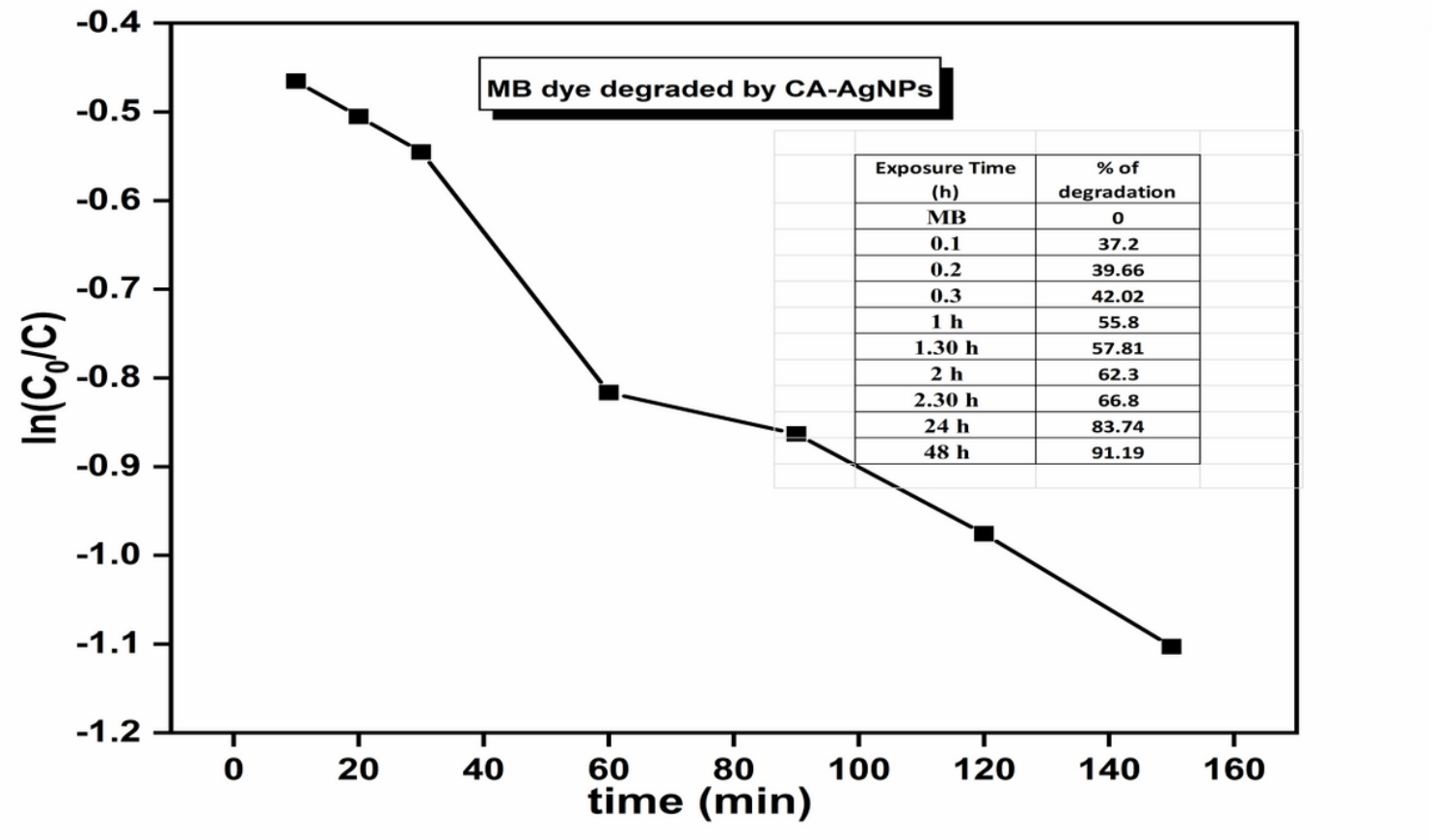

Exposure Time (h)	% of degradation
MB	0
0.1	37.2
0.2	39.66
0.3	42.02
1 h	55.8
1.30 h	57.81
2 h	62.3
2.30 h	66.8
24 h	83.74
48 h	91.19

Figure 8

Plot of bio-synthesized CA-AgNPs- $\ln(C_0/C)$ vs time

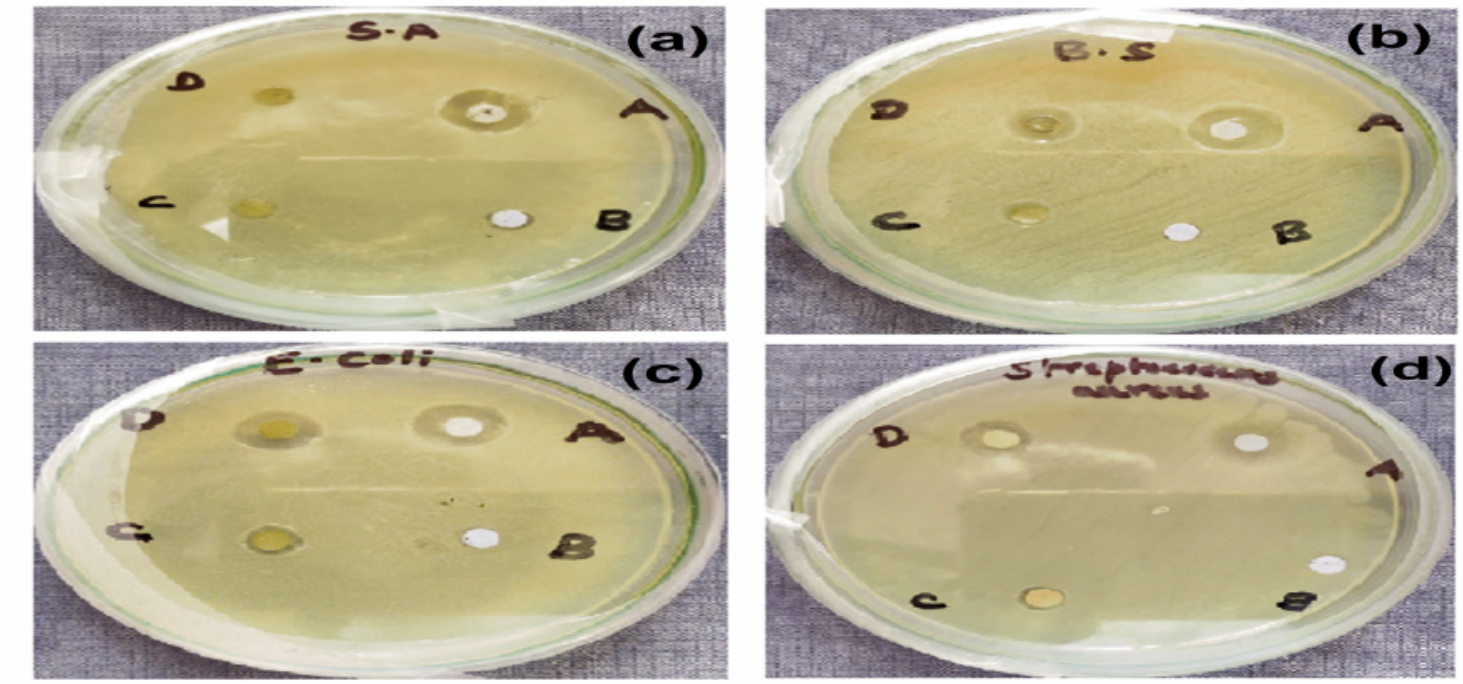

Figure 9

Anti-bacterial activities of bio-synthesized CA-AgNPs with various bacteria

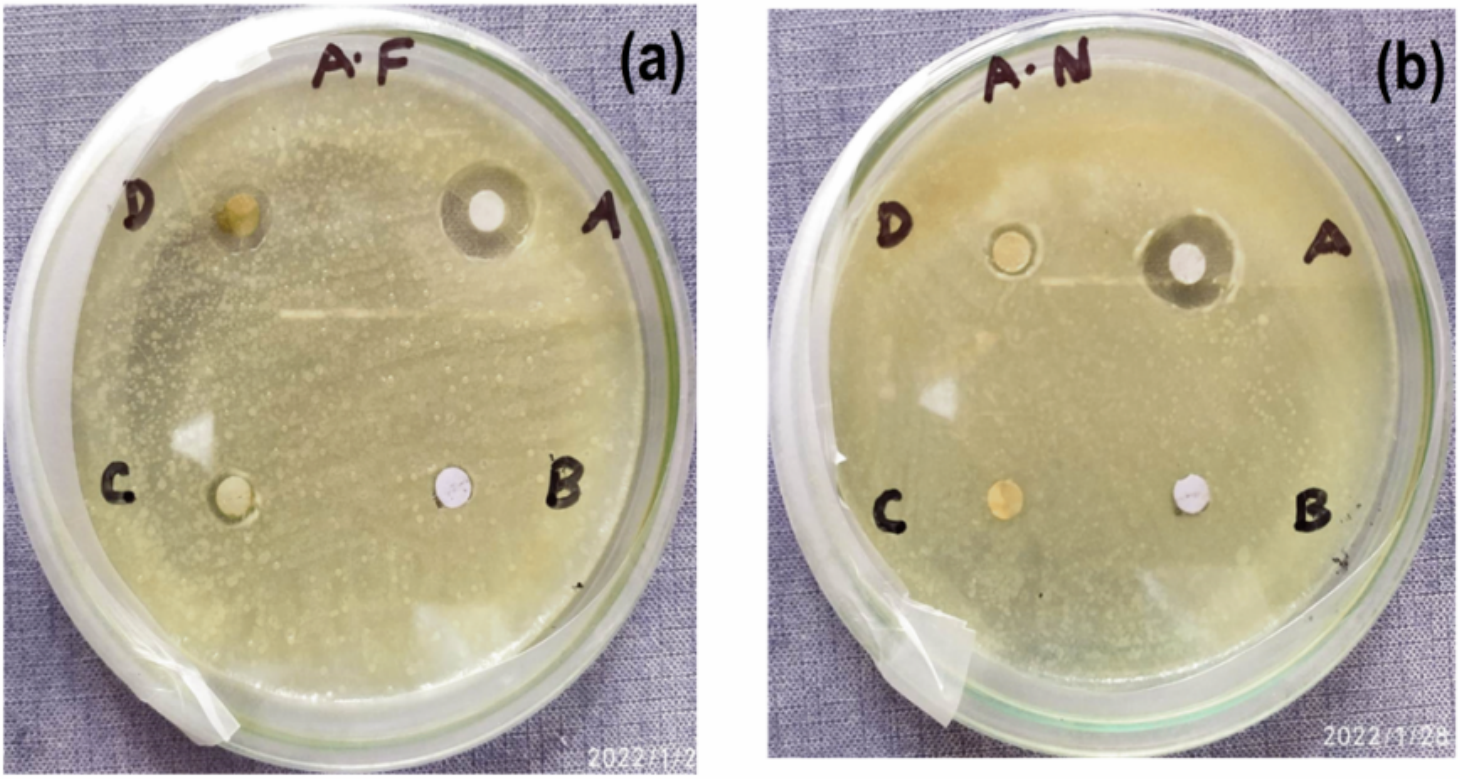

Figure 10

Anti-fungal activity of bio-synthesized CA-AgNPs with (a) *Aspergillus flavus* and (b)

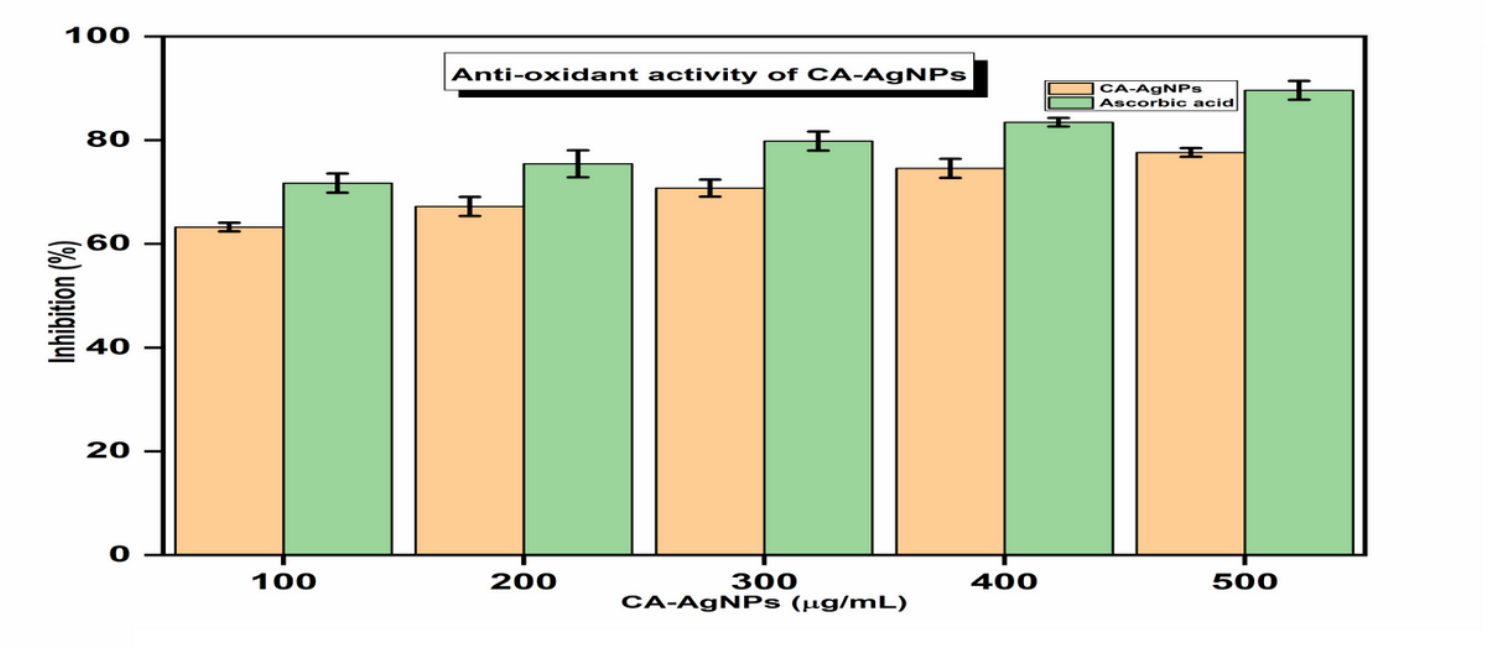

Figure 11

Anti-oxidant activity bar diagram of bio-synthesized CA-AgNPs.

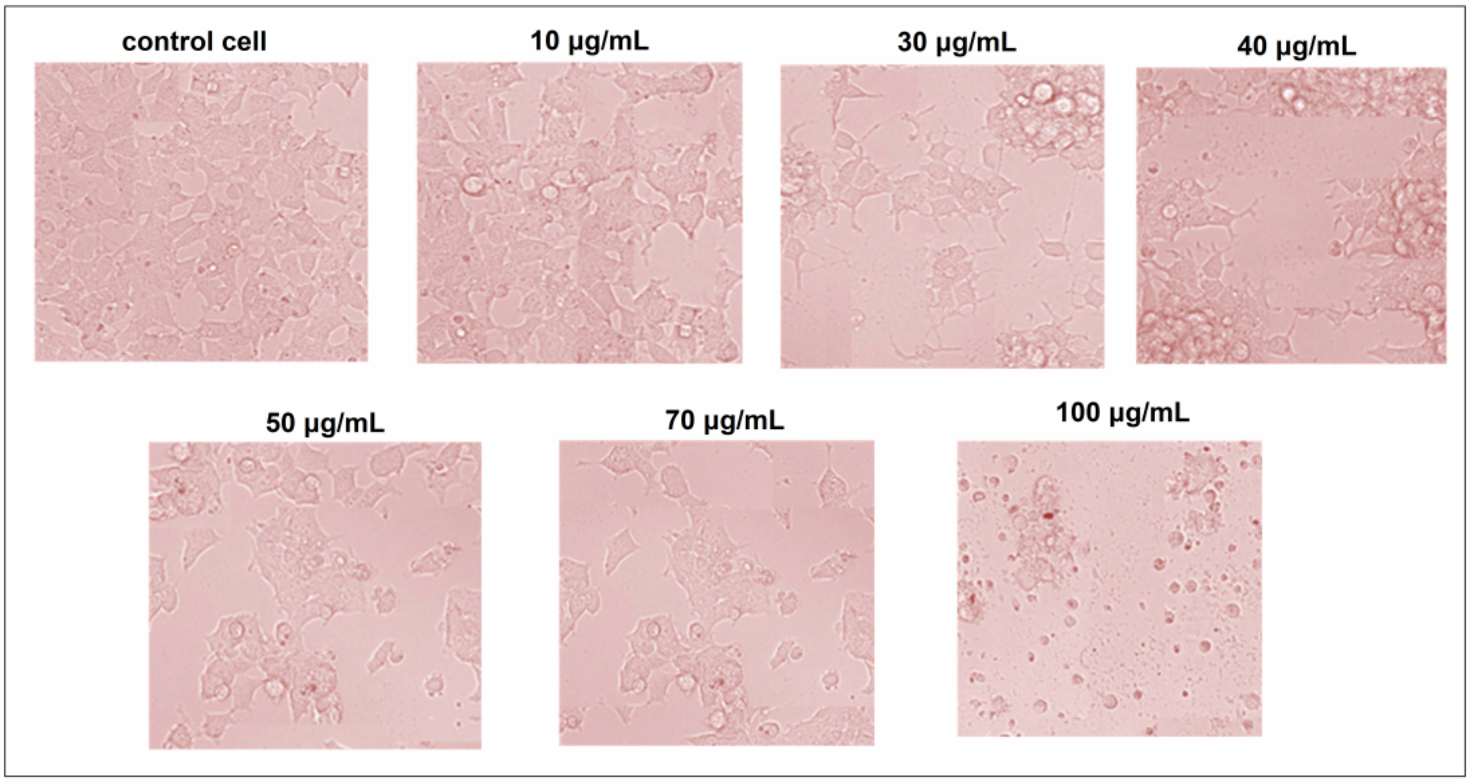

Figure 12

Cytotoxicity activity of bio-synthesized CA-AgNPs with various concentration with MCF-7 cells.

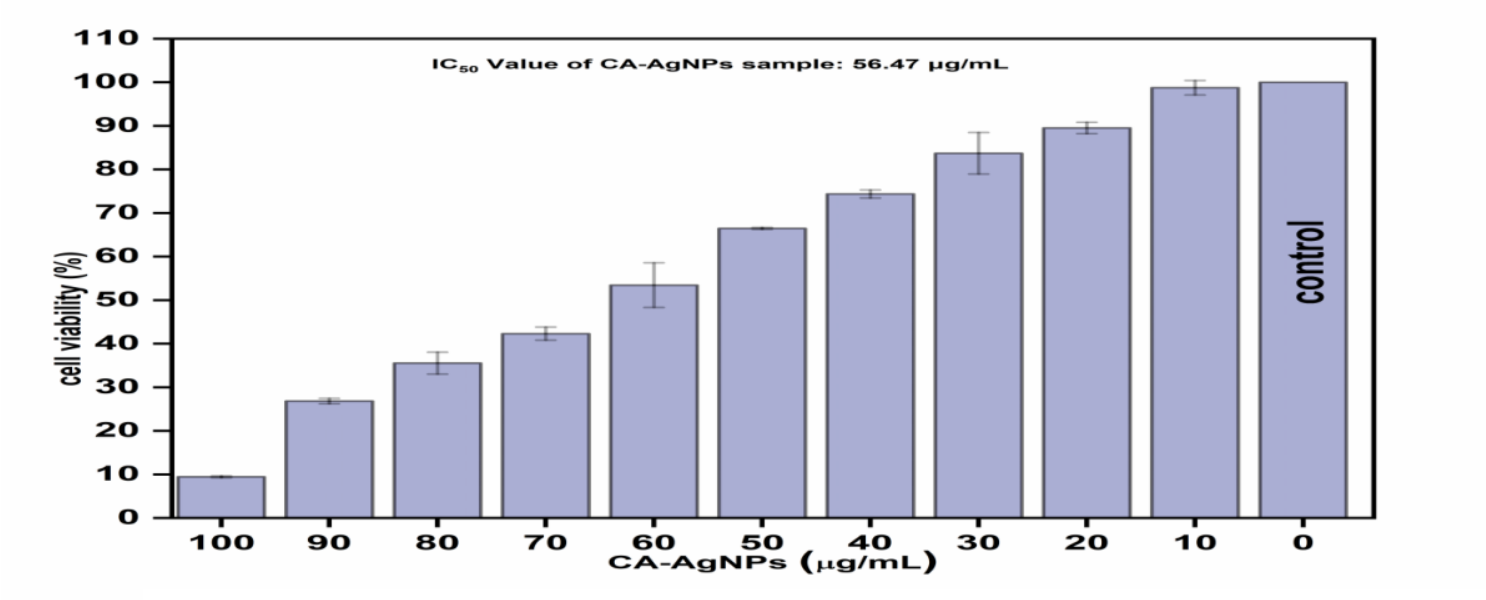

Figure 13

Cell viability percentage of bio-synthesized CA-AgNPs